On the Nuclear Capture of Muons with Electron Emission

M. CONVERSI, L. DI LELLA, A. EGIDI, C. RUBBIA,* AND M. TOLLER
Istituto di Fisica dell'Università-Sezione di Roma dell'I.N.F.N., Roma, Italy
(Received December 15, 1960)

Two experiments carried out to search for the process of muon capture with electron emission are reported. The second of the two experiments is nearly 200 times more sensitive than earlier attempts to find this capture mode, but no indication is obtained in favor of the latter. In both experiments negative muons are made to stop in copper, where coherent capture is predominant, so that the "capture electrons" should be emitted with an energy spectrum sharply peaked around 100 Mev. For the branching ratio of the process searched for, relative to ordinary muon capture, upper limits of about 5×10^{-6} and 5×10^{-6} are established through the first and second experiment, respectively.

1. INTRODUCTION

NO satisfactory interpretation exists of the experimental fact that the processes

$$\mu^+ \rightarrow \epsilon^+ + \gamma, \tag{1}$$

$$\mu^+ \rightarrow e^+ + e^- + e^+, \tag{2}$$

$$\mu^- + N \rightarrow N + e^-, \tag{3}$$

have been searched for as yet unsuccessfully. None of these processes, indeed, is incompatible with any of the well-established conservation laws upon which any present theory of the elementary particles is based. One is thus led to think that if some selection rule holds, its origin must be found in some peculiar feature of the structure of the interaction governing the processes in question. The absence of processes (1), (2), and (3) might be understood, for example, if the interaction is rigorously local or also if two types of neutrino exist.[1] On account of the now generally accepted "universality" of the Fermi interactions, the failure in the attempts to observe these processes involves the whole field of the weak interactions, even if exhibited in reactions involving specifically the muon. Under these circumstances it is clearly of great interest to establish the degree of "forbiddenness" of these unobserved processes, through accurate measurements capable of yielding upper limits as small as possible for their branching ratios relative to the corresponding ordinary processes [$\mu^+ \rightarrow e^+ + \nu + \bar{\nu}$ for the case of reactions (1) and (2) and $\mu^- + p = n + \nu$ for the case of (3)].

Upper limits of the order of 10^{-6} and 10^{-5}, respectively, have been established[2,3] for the case of reactions (1) and (2). In the first search for process (3) cosmic-ray muons were utilized.[4] More recently, in an experiment one hundred-fold more sensitive, carried out at the Nevis cyclotron, in which the muons were stopped in a Cu target,[5] an upper limit of about 10^{-3} has been established for the branching ratio

$$R = \frac{\text{Rate of process } \mu^- + \text{Cu} \rightarrow \text{Cu} + e^-}{\text{Rate of process } \mu^- + \text{Cu} \rightarrow \text{Ni} + \nu^-}. \tag{4}$$

Apart from the fact that the present status of the theory of weak interactions demands a close examination of all possible modes of decay and capture of the muon, a further investigation of process (3) appears useful from the following considerations. Reactions (1), (2), and (3) can be interpreted in terms of a hypothetical Feynman diagram of the type shown in Fig. 1, where the "box" contains the unknown structural properties of the interaction. More precisely, such a diagram represents process (1) if the emitted photon is real. If a virtual photon is emitted which converts internally into an $(e^+ - e^-)$ pair, the diagram represents process (2). Process (3) can be also represented by the same diagram if the virtual photon is absorbed by the nucleus responsible for the muon capture. It has been shown by Weinberg and Feinberg,[6] and independently by Cabibbo and Gatto,[7] that the matrix elements relative to these three processes can be written down on a phenomenological basis, without attachment to any specific property of the structure of the interaction "contained" in the box of Fig. 1. These authors have also pointed out that even if the mechanism of the interaction has properties for which no real photon can be emitted [so that process (1) is forbidden], still processes (2) and (3), in which a virtual photon is produced, might exist at a level experimentally accessible. Thus the observed absence of process (1) tells us nothing concerning the possible existence of processes (2) and (3). A more detailed analysis of the problem shows,[8]

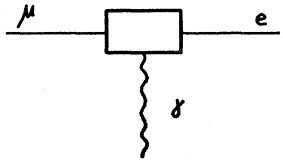

FIG. 1. Feynman diagram for process $\mu \rightarrow e + \gamma$. It also represents the capture process $\mu^- + N \rightarrow N + e^-$, if γ is a virtual photon absorbed in the Coulomb field of the capturing nucleus.

* Now at CERN, Geneva, Switzerland.
[1] M. Gell-Mann, Revs. Modern Phys. **31**, 834 (1959).
[2] D. Berley, J. Lee, and M. Bardon, Phys. Rev. Letters **2**, 357 (1959); J. Ashkin, T. Fazzini, G. Fidecaro, N. H. Lipman, A. W. Merrison, and J. Paul, Nuovo cimento **14**, 1266 (1959).
[3] J. Lee and N. P. Samios, Phys. Rev. Letters **3**, 55 (1959).
[4] A. Lagarrigue and C. Peyrou, Compt. rend. **234**, 1873 (1952).
[5] J. Steinberger and H. B. Wolfe, Phys. Rev. **100**, 1490 (1955).
[6] S. Weinberg and G. Feinberg, Phys. Rev. Letters **3**, 111 and 244 (1959).
[7] N. Cabibbo and R. Gatto, Phys. Rev. **116**, 1334 (1959).
[8] F. J. Ernst, Phys. Rev. Letters **5**, 478 (1960).

furthermore, that for a given sensitivity of the experimental device, more information can be derived searching for process (3) rather than for process (2).

Contrary to the case of ordinary muon capture, no change in the atomic number Z of the capturing nucleus occurs as a consequence of process (3). If after absorbing the virtual photon of Fig. 1 the capturing nucleus remains in its ground state, then the capture mode is *coherent*, the unchanged nucleus participating as a whole in the capture process. In this case the electron is emitted always with the same energy, which for a Cu nucleus turns out to be 103.8 Mev. An *incoherent* capture mode occurs, instead, when the nucleus goes into an excited state after absorbing the virtual photon. Then the energy of the emitted electron depends on the excitation energy of the nucleus. The energy spectrum of these "capture electrons" has been calculated by Steinberger and Wolfe[5] using for the nucleus the Chew-Goldberger model.[9] This spectrum exhibits a maximum at about 93 Mev and yields an average energy of nearly 85 Mev.

The relative weight of the two possible capture modes has been calculated for various nuclei,[6,7] making use of electromagnetic form factors known experimentally. The ratio of the probabilities of the coherent to the incoherent mode is found to have a maximum of at least 6 around the value $Z=29$. This is a first reason to choose Cu as a target to stop the negative muons. From an experimental point of view it is indeed evident that a close investigation of process (3) is made difficult by the presence of decay electrons arising from negative muons which have escaped nuclear capture. Apart from small effects due to the motion of the muon in the Bohr orbit,[10] the decay electrons have a maximum energy of about 53 Mev which is only slightly more than half the energy of the monoenergetic electrons arising from the coherent capture mode. A sharp separation between decay and capture electrons can be achieved, therefore, if the coherent mode of capture is predominant with respect to the incoherent mode in which also low-energy electrons are present. A second reason to choose Cu as a target to stop the muons is that this material represents a convenient compromise between the desirability of high Z, in order to have a large fraction of μ^- captured and, at the same time, of low Z, in order to have a small probability of radiation losses for the electrons emitted from the target.

Two experiments have been carried out by us at the CERN synchrocyclotron to search for process (3). No indication has been obtained in favor of the existence of such a process. In the first experiment, described in the following section, the sensitivity is increased by a factor of ~ 20 with respect to the last experiment reported on the subject.[5] With a further increase of a factor ~ 10 in sensitivity, the second experiment (Sec. 3) yields an upper limit of about 5×10^{-6} for the branching ratio (4). Measurements of the efficiency of the electron telescopes used in the two experiments are reported in Sec. 4. The results of the experiments, partly reported and published,[11] are given in Sec. 5. In the last section they are discussed and compared with those recently obtained by Sard, Crowe, and Kruger[12] in a very accurate experiment on the same problem, performed with a different technique.

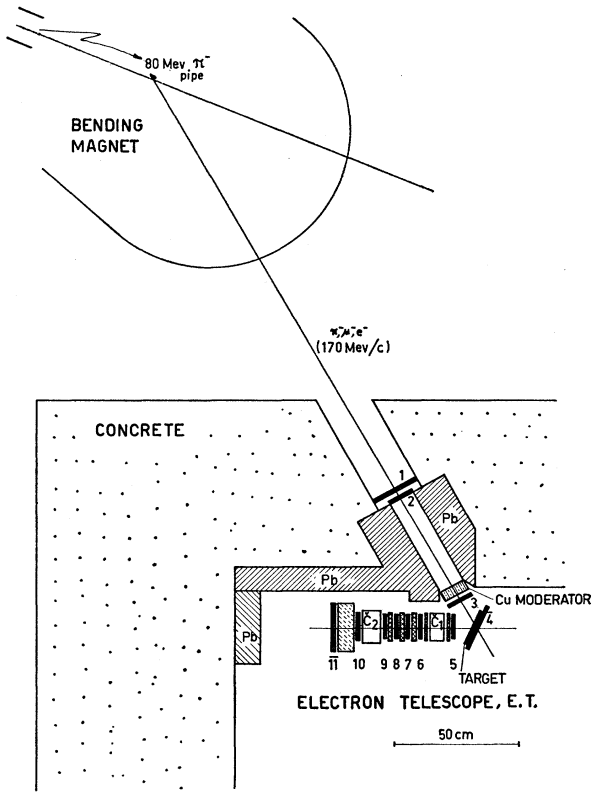

FIG. 2. Experimental arrangement in the first experiment. Counters 1, 2, $\cdots$ 11 are plastic scintillators 1.25 cm thick; $\check{C}_1$ and $\check{C}_2$ are Čerenkov counters. The absorber between counters 10 and 11 is an Al block 8 cm thick. All other absorbers in ET are made of compressed graphite. An event of the type searched for would appear as a μ^- stop ($S=1\cdot 2\cdot 3\cdot \bar{4}$) followed by the emission of an energetic electron capable of producing an anticoincidence of the type $B(B=5\cdot\check{C}_1\cdot 6\cdots\check{C}_2\cdot 10\cdot\bar{1}\cdot\bar{1}\bar{1})$.

2. ARRANGEMENT IN THE FIRST EXPERIMENT

Taking advantage of the possibility of running simultaneously more experiments in the "neutron room" of

[9] G. F. Chew and M. L. Goldberger, Phys. Rev. **77**, 471 (1950).

[10] L. Tenaglia, Nuovo cimento **13**, 284 (1959); H. Überall, Nuovo cimento **15**, 163 (1960).

[11] M. Conversi, L. di Lella, A. Egidi, C. Rubbia, and M. Toller, Nuovo cimento **18**, 1283 (1960). Reported also at the Naples Congress of the Societá Italiana di Fisica, September, 1960 (unpublished); and by V. Telegdi at the *Proceedings of the 1960 Annual International Conference on High-Energy Physics at Rochester* (Interscience Publishers, New York, 1960).

[12] R. D. Sard, K. M. Crowe, and H. Kruger, Phys. Rev. **121** 619 (1961). Reported also at the *Proceedings of the 1960 Annual International Conference on High-Energy Physics at Rochester* (Interscience Publishers, New York, 1960).

the CERN synchrocyclotron, our first experiment was carried out in parallel with others, using the pion pipe of 80-Mev nominal energy. As shown in Fig. 2, the beam from this pipe goes through an analyzing magnet which bends its charged component with momentum around 170 Mev/c into a Pb collimator. The beam of negative particles thus obtained contains about one muon and three electrons per ten pions entering the Pb collimator. Pions of momentum 170 Mev/c have a residual range ($\sim$28 g/cm^2 in Cu) smaller than that of muons of the same momentum. For a proper choice of the thickness of the Cu moderator placed just before counter 3 they get absorbed, while the muons reach the target. The stop of a charged particle in the target is electronically defined by an anticoincidence $1\cdot2\cdot3\cdot\bar{4}$ among the plastic scintillators 1,2,3 (used in coincidence) and 4 (in anticoincidence). An event $1\cdot2\cdot3\cdot\bar{4}$ will be indicated by the letter S ("stop"). The rate of the anticoincidences S was measured for different thicknesses of the Cu moderator. From the range curves thus obtained the thickness of the Cu moderator giving a maximum of muon stops in the target was determined. The target used in the measurements just mentioned, as well as in the main experiment, was a Cu sheet of area 12×17 cm^2, 0.5 cm thick, placed at about 35° to the beam direction. Under these conditions the average rate of muon stops in the target was $\sim$500 particles/sec, corresponding to nearly half the intensity of the incident muons.

Only a fraction $f=0.92$ of the stopped μ^- mesons undergo nuclear capture in Cu, while the remaining 8% decay with a lifetime of 160 nsec,[13] emitting electrons of maximum energy of about 53 Mev. On account of the rarity of process (3), it is important that the experimental device be as insensitive as possible to these electrons which might otherwise contribute to the background of spurious events simulating the "capture electrons" searched for. At the same time the device must have a reasonably good efficiency for the detection of the latter. These requirements are satisfactorily fulfilled making use of the electron telescope (ET) of Fig. 2 which, as will be seen later (Sec. 4), has an efficiency of the order of 10^{-6} for the decay electrons and an efficiency $\epsilon\approx0.15$ for the capture electrons, thus enabling an extremely sharp separation between these two types of electrons. This telescope is made up of two Čerenkov counters ($\check{C}_1$ and $\check{C}_2$) and six plastic scintillators (5,6$\cdots$10), all in coincidence among themselves and in anticoincidence with a seventh plastic scintillator, 11.

Graphite absorbers 1 or 2 cm thick are also inserted in ET, as shown in the figure. Adding the thicknesses of the six coincidence plastic scintillators (1.25 cm each) of $\check{C}_1$ (5 cm of Lucite[14]), of $\check{C}_2$ (6 cm of Lucite), and of the material surrounding all these counters, one finds that from the center of the target to the center of counter 10 there is a total of $\sim$37 g/cm^2 of carbon equivalent. An electron of $\sim$50 Mev has a small but still appreciable probability to cross such a thickness since it may travel partly as a bremsstrahlung photon which later converts into an electron pair. The reason for using so many counters in ET is then clear: it has the purpose to minimize the probability of detecting a decay electron which might cross part of ET as electromagnetic radiation. For the same purpose low-Z material (compressed graphite) has been chosen for the absorbers inserted in ET, in each of which electrons have a comparatively low probability to radiate, though losing an appreciable fraction of their energy by ionization. Compressed graphite has also the advantage of a comparatively large density (2.04 g/cm^3), so that its total thickness can be made large enough to achieve a drastic elimination of the decay electrons without excessive reduction in the effective solid angle, ω, of ET seen from the target.

In addition to the decay electrons, another source of spurious events can arise from the background of cosmic rays and of particles present around the machine. To reduce this source several precautions were taken:

(1) The apparatus was surrounded by thick blocks of heavy concrete and lead, as schematically shown in Fig. 2.

(2) In order to exclude any contamination from events simultaneous with the arrival of a particle of the beam, also counter 1 was placed in anticoincidence, to form an "8-fold" anticoincidence of the type $B=(5\cdot\check{C}_1\cdot6\cdots\check{C}_2\cdot10\cdot\bar{1}\cdot\bar{11})$. Such a contamination might arise, for example, from an electron of the beam scattered from the target into ET.

(3) It was required that the B pulse followed a pulse S within the time interval $\Delta\theta$ from $\sim$15 to 430 nsec, to form an event $BS_{\rm del}$. The choice $\Delta\theta=\sim415$ nsec is reasonable, corresponding to $\sim$2.6 μ^- lifetimes in Cu ($\tau_{\rm Cu^-}=160$ nsec). The fraction of delayed events thus accepted is $u=\exp(-15/160)\times[1-\exp(-2.60)]=0.84$.

(4) In order to reduce to a negligible value a possible contribution to the background from the cosmic radiation, events $BS_{\rm del}$ were recorded only if occurring during the machine bursts. Subject to rather large fluctuations, the average duration of the machine bursts was around 400 μsec.

If D is the duty cycle of the synchrocyclotron and n_S, n_B represent the rates of events S and B, respectively, the rate of accidental events $BS_{\rm del}$ is clearly $n_Sn_BD\Delta\theta$. For a given duty cycle of the machine and for the choice $\Delta\theta=2.6\tau_{\rm Cu^-}$, reduction of the accidental rate without a corresponding reduction in the rate of the possible genuine events $BS_{\rm del}$ (which is essentially proportional to n_S) must be achieved by making n_B as small as possible. This explains the reason for including in ET two Čerenkov counters and the anticoincidence counter 11. Indeed, the Čerenkov counters prevent all

[13] J. C. Sens, Phys. Rev. **113**, 679 (1959).

[14] Lack of scintillating properties was checked for this material in preliminary measurements carried out in Rome using slow cosmic-ray muons.

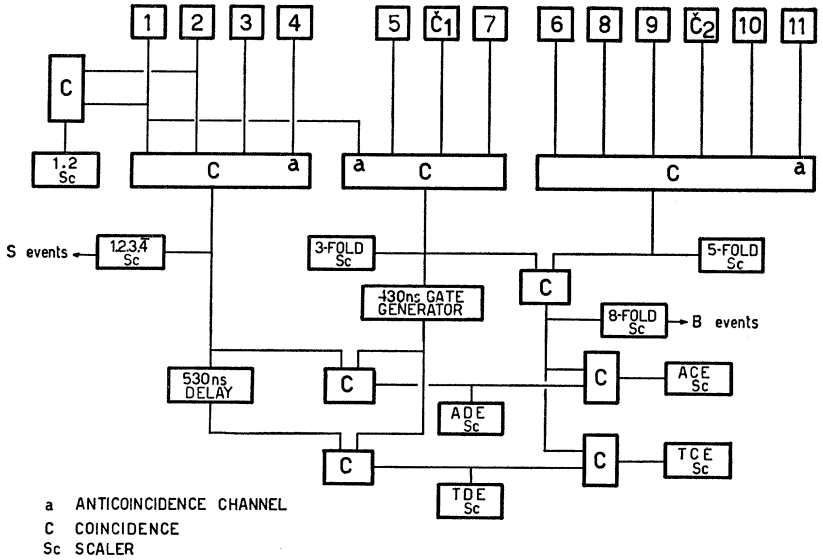

FIG. 3. Simplified block diagram of the electronics used in the first experiment to record the events listed in Table I.

unwanted slow particles from being detected, while the anticoincidence counter 11, at the end of ET, excludes fast cosmic-ray muons, as well as energetic electrons not originating in the target. On the other hand, a capture electron emitted from the target within the solid angle ω of ET is usually unable to reach the anticoincidence counter 11, because of the 8 cm thick Al block placed between counters 10 and 11. Counter 11, therefore, causes only a small reduction ($\sim 10\%$, see Sec. 4) in the detection efficiency of ET for the capture electrons.

Many different types of events were recorded electronically in the way shown by the simplified block diagram of Fig. 3. These events are listed and explained in Table I where examples of the corresponding physical events are also given. The recording of so many types of events during the performance of the experiment has proved to be of great utility, enabling us to maintain the whole apparatus continuously under control. In particular, from the relation

$$\frac{\text{Rate of ADE}}{\text{Rate of 3-fold}}=\frac{\text{Rate of ACE}}{\text{Rate of } B}, \tag{5}$$

one can determine with good accuracy the rate of accidental AB_{del} (indicated for brevity as ACE: "accidental capture electrons") from the measured rates of ADE ("accidental decay electrons"), 3-fold, and B events (see Fig. 3 and Table I for the meaning of the symbols). On account of the rarity of these accidental events (only one event recorded in the whole experiment) their rate would be determined with very poor accuracy from the number recorded at the output ACE of Fig. 3, which is nevertheless useful for a check of the internal consistency of the results. It should also be pointed out that the determination of the rate of ACE from Eq. (5) is independent of the time structure of the beam, which is subject to considerable changes during the operation of the machine.

If genuine capture electrons exist at a rate experimentally accessible, they should appear outside of the

TABLE I. List of events electronically recorded in the first experiment (see also Fig. 3). Numbers from 1 to 11 refer to the plastic scintillators of Fig. 2. In the first column of the table, a line above a number means that the corresponding counter is used in anticoincidence. Abbreviations used in the second column are: E for "electron," D for "decay," C for "capture," T for "total," and A for "accidental." The difference TDE-ADE gives the genuine decay electrons capable to reach counter 7. Apart from a possible spurious contribution due to the decay electrons, the difference TCE-ACE gives the genuine capture electrons searched for. In the whole experiment, 3 events of the category TCE and 1 of the category ACE have been recorded.

Recorded event	Symbol	Explanations
$1\cdot 2$		Recorded as "monitors."
$1\cdot 2\cdot 3\cdot \bar{4}$	S	Typical event: μ^- stop in the target.
$5\check{C}_1 7\cdot \bar{1}$	3-fold	Typical event: decay electron reaching at least counter 7 of ET.
(3-fold)$\cdot S_{\text{delayed}}$	TDE	Typical event: (a) process $\mu^-=e^-+\nu+\nu$; (b) accidental coincidence of a 3-fold with an event S.
(3-fold)$\cdot S$	ADE	Typical event: accidental coincidence of a 3-fold with an event S.
$5\check{C}_1 6\cdot 7\cdot 8\cdot 9\cdot \check{C}_2 10\cdot \bar{11}\cdot \bar{1}$	B	Typical event: electron from the target side stopping in the Al block between counters 10 and 11.
BS_{delayed}	TCE	Typical events: (a) process $\mu^-+N=N+e^-$; (b) accidental coincidence of events S and B.
BS	ACE	Typical event: accidental coincidence of events S and B.
$6\cdot 8\cdot 9\cdot C_2 10\cdot \bar{11}$	5-fold	Recorded for a check of the internal consistency.

statistical errors in the difference between the recorded numbers of "total" and "accidental capture electrons" (TCE-ACE). The small difference observed in this first experiment (Sec. 5) is of no statistical significance.

3. ARRANGEMENT IN THE SECOND EXPERIMENT

The high-intensity beam of low-energy muons recently developed at the CERN synchrocyclotron[15] has been used throughout our second experiment. This beam is obtained by injecting the pions produced in the internal target of the synchrocyclotron into a magnetic channel made up of 24 quadrupole lenses. The latter concentrate the muons arising from the decay of the pions along their path. At the end of the magnetic channel, muons of smaller energy are bent by a deflecting magnet into a beam which, under the conditions of operation used by us, has the following characteristics: Average muon energy ~60 Mev; less than 5% pion plus electron contamination; intensity and energy spread such as to allow the stopping of 3700 muons/sec on an area of 100 cm², in a Cu target 0.5 cm thick placed at 45° to the beam direction, at a distance of 1.1 m from the exit of the bending magnet.

The apparatus, reproduced schematically in Fig. 4, is similar to the one used in the first experiment, though its "electron telescope" (ET) contains only one Čerenkov counter and a greater number of plastic scintillators. The larger number of counters in coincidence and the different distribution of the graphite absorbers make it possible to achieve a further reduction in the probability of detecting spurious events due to decay electrons from μ^- mesons which have escaped nuclear capture in the Cu target. Moreover, in order to minimize the contribution to the background from spurious events of accidental origin, use has been made of two additional anticoincidence plastic scintillators, 11 and 12. The latter, not represented in Fig. 4, was placed horizontally above ET (for protection against cosmic-ray showers) separated from it by a 2 cm thick Pb layer.

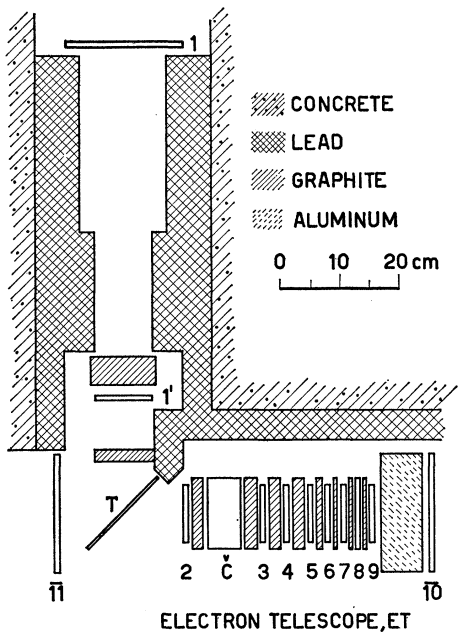

FIG. 4. Apparatus employed in the second experiment.

The simplified block diagram of Fig. 5 shows how the events selected by the apparatus of Fig. 4 were electronically recorded. On account of the small contamination and good energy definition of the beam, a coincidence $1\cdot1'$ between counters 1 and 1′ represents in general a muon stop in the target. Such a coincidence serves also as a monitor. The total number of muons actually stopped in the target during the whole experiment can be normalized to the number of monitors $1\cdot1'$ making use of the measurements taken for this purpose under the conditions explained in Table II.

Coincidences among the first n counters of ET, starting from $n=3$, are scaled if the following conditions are fulfilled: (1) They must not be accompanied within about 20 nsec by pulses from counters 1 and 11; (2) they must occur during the (~400 μsec long) machine bursts. In the following discussion we shall refer to events satisfying these conditions simply as 3-fold, 5-fold, 6-fold, . . . 9-fold anticoincidences.

The chief information given by the apparatus is recorded taking the pictures of an oscilloscope. More precisely, a 7-fold anticoincidence triggers the sweep of a Tektronix 545 *A* oscilloscope. Through suitable delays which serve to achieve a satisfactory spatial separation in the pictures, the negative pulses from counters 7, 8, 9, 10, and 12, as well as the positive pulse from the coincidence $1\cdot1'$, are displayed on the oscilloscope sweep. A picture in which all pulses are present appears as in Fig. 6. The oscillogram corresponding to an event of the type searched for should not contain pulses from

TABLE II. Results of measurements to determine the number of μ^--stops per monitor $1\cdot1'$ in the second experiment. The measurements have been taken without graphite absorbers in the electron telescope of Fig. 4, using a graphite target equivalent to the Cu target of the main experiment. Under these conditions, the efficiency of the system of counters (2, Č, and 3) used to form a 3-fold coincidence can be estimated as 0.64 from pre-existing measurements.[a] Such a system accepts electrons emitted from the target within an average solid angle of ~0.19 steradian. From the data reported in the first and second columns, one then finds 0.4 μ^- stops per monitor $1\cdot1'$. Similar measurements have been taken also in the first experiment, giving 4.41×10^{-2} μ^- stops per monitor $1\cdot2$. Since 3.70×10^9 monitors $1\cdot2$ were recorded, one gets $N=1.63\times10^8$ for the total number of μ^- stopped during the first experiment.

	Type of event	$1\cdot1'$	3-fold	5-fold	6-fold	7-fold	8-fold	9-fold
No. of events	with C target	1238×10^3	5192	1679	1053	514	377	288
	without target	2881×10^3	841	214	140	80	57	37

[a] S. Lokanathan and J. Steinberger, Suppl. Nuovo cimento 2, 151 (1955).

[15] A. Citron *et al.*, Berkeley Meeting, September, 1960 (unpublished).

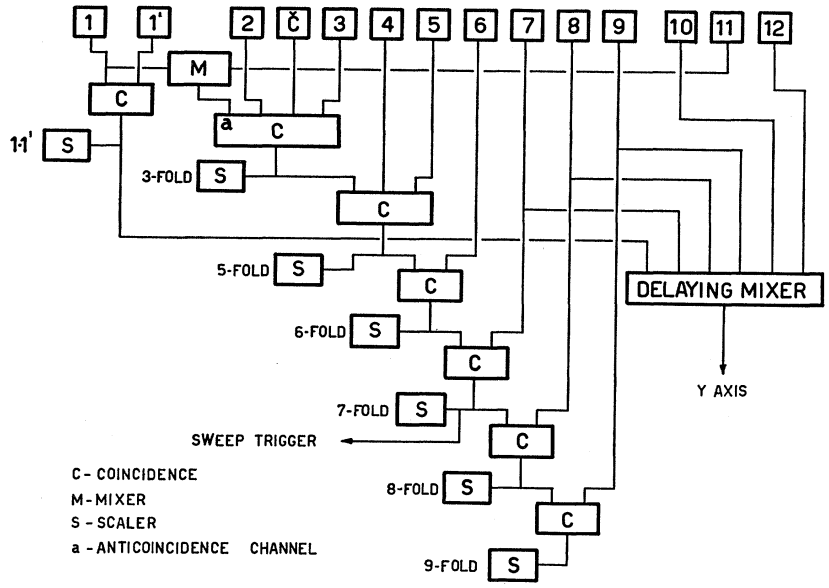

FIG. 5. Simplified block diagram of the electronics used in the second experiment.

counters 10 and 12, whereas there should be pulses from counters 7, 8, and 9, as well as the pulse from the coincidence $1\cdot1'$. The latter, furthermore, should be in such a position as to indicate a muon stop followed by the corresponding capture electron within the time interval from 15 to 500 nsec. This last condition reduces the number of recorded events to a fraction $u=\exp(-15/160)[1-\exp(-485/160)]=0.87$.

4. EFFICIENCY OF THE ELECTRON TELESCOPES

For a given value R of the branching ratio (4) and for a total number N of μ^- mesons stopped in the target, the expected number of events due to both genuine and spurious capture electrons, is given by

$$m(R)=aR+b, \tag{6}$$

where

$$a=Nfu\epsilon(\omega/4\pi); \tag{7}$$

ϵ is the detection efficiency of the electron telescope, and b represents the expected background of spurious events.

Rather than calculating it by a Monte Carlo method, we have preferred to make an experimental determination of the efficiency ϵ of the electron telescopes for the capture electrons. This determination becomes possible for both experiments, if the efficiency of the electron telescope used in the second experiment is measured with monoenergetic electrons of various energies. The electron beam necessary for these measurements was obtained by letting the external proton beam of the synchrocyclotron strike a Pb target and selecting, by means of two analyzing magnets, the particles produced with momenta in a narrow interval. Calibration of the selected momentum, corresponding to given values of the magnetizing currents, was based on the floating-wire technique.

TABLE III. Results of measurements of the efficiency of the electron telescope used in the second experiment. These measurements have been taken without the anticoincidence counters (10 and 11, see Fig. 4), using monochromatic electrons of various energies (first column) filtered through Cu sheets of various thicknesses (second column). Only statistical errors are indicated. The numbers of 3-fold coincidences have been calculated as explained in the text.

E (Mev)	Cu thickness (mm)	Percentage efficiency 3-fold	5-fold	6-fold	7-fold	8-fold	9-fold
70	4	67	15±1	5.3±0.6	2.2±0.4	0.6±0.2	0.17±0.09
80	4	71	24±1	11.8±0.9	6.3±0.6	2.7±0.4	1.1 ±0.2
90	4	75	32±2	19±2	12.6±1.2	7.8±0.9	4.0 ±0.6
100	0	91	61±2	46±2	36±2	29±1	20.5 ±1.0
100	2	86	52±2	38±2	28±1	18.6±1.0	13.8 ±0.8
100	4	78	39±2	26±1	19.1±0.9	12.9±0.7	8.4 ±0.5
100	6	70	29±1	18±1	11.1±0.6	7.1±0.5	4.2 ±0.3
110	4	81	45±2	32±2	24.7±1.2	18.2±1.0	11.9 ±0.7

For some of the selected energies the measurements of efficiency were performed by interposing along the path of the electron beam, before ET, Cu sheets of small thickness, in order to see the effect of the energy losses suffered by the electrons in the Cu target.

The results of these measurements are given in Table III. The efficiency relative to the 3-fold coincidences has been calculated. Allowance has not been made, in these calculations, for the fact that the ionization losses, reducing the electron energy, have an influence on the radiation losses. In this approximation—

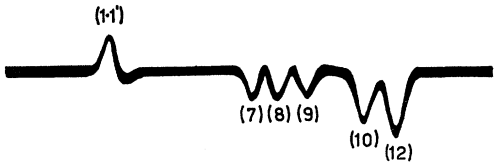

FIG. 6. Reproduction of an oscillogram containing the pulses of all counters.

which appears legitimate from the consistency of the efficiencies calculated and measured, at the same energy of 100 Mev, for four different Cu thicknesses—the efficiency relative to the 3-fold coincidences has the following meaning: It represents the probability that an electron of energy E, undergoing only radiation losses in a thickness of X radiation lengths, remains with an energy greater than that, E_j, lost in the same thickness by ionization only. This probability is given by[16] $[X-1, \ln(E/E_j)]!/\Gamma(X)$.

The curves of Fig. 7 refer to an interposed Cu thickness of 4 mm, corresponding to nearly half the target (one must remember that in the second experiment the latter was at 45° to the average direction of the electrons emitted in ET). The curves are relative to 7-fold, 8-fold, and 9-fold coincidences (recorded *without* the anticoincidence counters). In the actual experiment the presence of the anticoincidence counter 10 causes an appreciable reduction in efficiency because of the development of the electrophotonic cascade which may occasionally penetrate the whole Al absorber. Using 100-Mev electrons filtered through a 4-mm thick Cu sheet, we have measured the percentage of 8-fold coincidences accompanied by a pulse of counter 10. Under these conditions we have found a reduction in efficiency of nearly 10%.

From the curve of Fig. 7 relative to the 8-fold coincidences and taking into account the 10% reduction in efficiency due to counter 10, one finds that the efficiency for electrons produced in the target with the energy spectrum resulting from a mixture 6:1 of coherent and incoherent capture (Sec. 1) is given by

$$\epsilon=0.14, \text{ (for 8-fold in second experiment).} \quad (8)$$

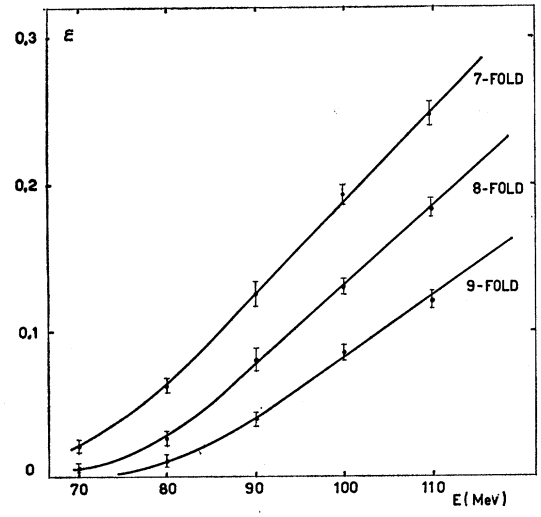

FIG. 7. Efficiency of the electron telescope ET of Fig. 4 for electrons of the energy indicated in abscissa, filtered through a 4 mm thick Cu sheet.

[16] W. Heitler, *Quantum Theory of Radiation* (Clarendon Press, Oxford, 1936), p. 226.

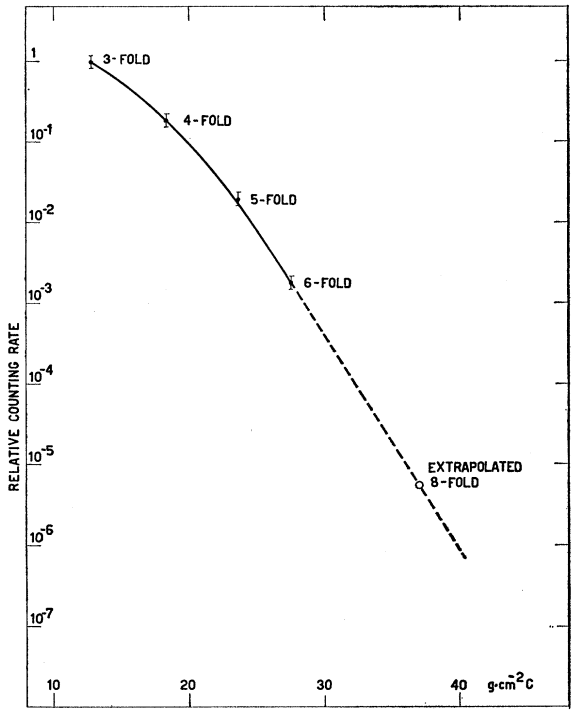

FIG. 8. Relative rate of n-fold coincidences among the first n counters of the electron telescope of Fig. 2. The 8-fold rate is arbitrarily extrapolated as shown in the figure, merely to indicate the smallness of the contribution deriving from the decay electrons.

By a reasonable interpolation of the data contained in Table III, for the electron telescope used in the first experiment one finds similarly

$$\epsilon=0.15 \text{ (for first experiment).} \quad (9)$$

No direct determination has been made of the detection efficiency of the telescopes for electrons arising from the decay of μ^- mesons which have escaped nuclear capture. From the results reported in the next section (Fig. 8) it appears, however, to be about 10^{-6} in both experiments.

5. RESULTS

For the interpretation of the experimental results we shall use the Poisson formula,

$$P(R)=(aR+b)^\nu/\nu!e^{(aR+b)}, \quad (10)$$

which represents the probability that the branching ratio has the value R, if ν events (genuine plus spurious) of the type searched for, have been actually observed when their expected number is given by Eq. (6).

In the course of our *first experiment*, consisting of nearly 200 runs of 30 minutes each taken in the conditions of Fig. 2, $\nu=3$ events have been recorded of the type TCE (see Table I). Correspondingly, $N=1.63\times10^8\mu^-$ stops occurred in the target, this figure being derived from the total number of recorded monitors 1.2 and from the measured number of μ^- stops

per monitor (see Table II). From the geometry of the apparatus used in the first experiment one finds $\omega/4\pi=7.5\times10^{-3}$. Inserting in Eq. (7) these figures, as well as the numerical values of f,u (Sec. 2), and ϵ [Eq. (9)], one obtains $a=1.35\times10^{5}$.

As pointed out in Sec. 2, the background rate is made up of a term deriving from the decay electrons and another term of accidental origin. Making use of Eq. (5) separately for each of the $\sim$200 runs, the latter is found to be 1.53 ± 0.27, in agreement with the fact that only one event ACE (Table I) has been recorded in the whole experiment. For an estimate of the former term, measurements have been taken of the n-fold coincidences among the first n counters of ET, with the results shown graphically in Fig. 8. Under the assumption that up to the 6-fold coincidences the bulk of the recorded counts is due to the decay electrons, the former term is estimated from the rate of 8-fold coincidences, extrapolated as shown in the figure, and from the requirement that such a coincidence follows a muon stop between 15 and 430 nsec (Sec. 2). We shall neglect this small term, thus making somewhat bigger the upper limit that we are going to establish for the branching ratio of the process sought.

The probability curve relative to our first experiment is plotted in Fig. 9, as graph 1, together with the curves relative to other experiments discussed below (see also Sec. 6). All graphs in Fig. 9 are normalized to 1 in their maxima and represent functions, $Q(R)$, which are proportional to those, $P(R)$, given by Eq. (10) for the appropriate values of the constants a,b,ν. Curve 1 contains the results of our first expriment: It shows in particular that above $R=5\times10^{-5}$, $Q(R)$ is $<\frac{1}{10}$. Hence, if coherent capture is 6 times more probable than incoherent capture [so that the value (9) of ϵ can be used], our first experiment yields

$$R<5\times10^{-5},$$

with 90% confidence level.

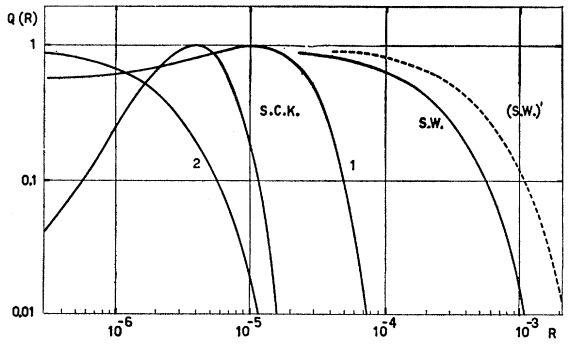

FIG. 9. Probability of the result obtained in each of the experiments indicated, as a function of the branching ratio R. Curve (S.W.)' refers to the result of the experiment of Steinberg and Wolfe interpreted as explained in the text; curve S.W. is relative to the result reported by the above-mentioned authors; curves 1 and 2 hold for our first and second experiment, respectively; curve S.C.K. for the experiment by Sard, Crowe, and Kruger.

TABLE IV. Results of the second experiment. From the number of monitors $1\cdot1'$ (first column) one obtains the total number N of μ^- stops ($N=6.26\times10^{8}$) using the results of Table II. "Good" n-fold anticoincidences ($n=3,5,6,\cdots9$) are characterized by the absence of pulses from counters 10 and 12 and by the presence of a pulse $1\cdot1'$ which indicates, with its position on the oscilloscope trace, that a μ^- stop is followed by electron emission between 15 and 500 nsec.

Type of event	$1\cdot1'$	3-fold	5-fold	6-fold	7-fold	8-fold	9-fold
Total number	1.56×10^{9}	207×10^{3}	695	62	33	18	7
"Good" n-fold anticoincidences	...	...	...	...	5	0	0

Table IV contains the results of our *second experiment*, consisting of $\sim$47 hours of effective measurements performed with the apparatus of Fig. 4 exposed to the muon beam mentioned in Sec. 3.

Since no "good" 8-fold anticoincidence has been recorded in the whole experiment, we shall use the value of ϵ given by Eq. (8) and, for the fractional solid angle relative to the 8-fold coincidences, the value $\omega/4\pi=5.5\times10^{-3}$ calculated from the geometry of the apparatus. From the total number of recorded monitors $1\cdot1'$ (Table IV, 2nd column) and from the number of μ^- stops per monitor (Table II) one finds $N=6.25\times10^{8}$ μ^- stops in the whole experiment. Since $f=0.92$ and in this case $u=0.87$ (Sec. 3), Eq. (7) yields $a=3.98\times10^{5}$.

Because of the negative result of this experiment ($\nu=0$), the probability $P(R)$ given by Eq. (10) is in this case equal to the product of the probability, $\exp(-aR)$, that no genuine event is recorded while the expectation value is aR, times the probability, $\exp(-b)$, that no spurious event is recorded while the expectation value is b. The information derivable from our second experiment is, therefore, independent of the expected background and the function $Q(R)=\exp(-3.98\times10^{5}R)$, plotted as curve 2 in Fig. 9, is suitable to represent the result. It is seen that

$$R<5.9\times10^{-6},$$

with 90% confidence level. As before, such a result, based on the use of Eq. (8), holds for coherent capture 6 times more probable than incoherent capture. In the case of purely incoherent capture the result depends of course on the energy left to the nucleus. If an average nuclear excitation energy of 15 Mev is assumed, one finds $\epsilon=0.06$, so that $R<1.4\times10^{-5}$.

It should be pointed out that in the course of both experiments the apparatus was continuously kept under control. In particular, measurements without graphite absorbers in the electron telescopes, ET's, were frequently taken. Under these conditions the decay electrons could penetrate into the ET's, and large numbers of n-fold coincidences among the first n counters of the telescopes were quickly collected even for the highest

values of n ($n=8$ for the first experiment and $n=9$ for the second).

The absence of 8-fold and 9-fold "good" anticoincidences among the events recorded in the second experiment (Table IV) is consistent, on the other hand, with an estimate of the expected background b. Indeed, a more detailed analysis of our data (including the pictures of the oscilloscope traces) leads to the conclusion that the expectation value of b in our second experiment is between 1 and 2 events.

6. DISCUSSION

In addition to the results of the two experiments described in this paper, Fig. 9 contains also in graphical form the final result reported by Steinberger and Wolfe[5] (curve S.W.) and that obtained by Sard, Crowe, and Kruger[12] (curve S.C.K.). The graph labelled (S.W.)′ in Fig. 9 is deduced from the experimental results of Steinberger and Wolfe: (a) assuming that coherent capture is 6 times more probable than incoherent capture; (b) interpolating from our measurements of Sec. 4 the correct value of the detection efficiency of the electron telescope used by these authors. Indeed this efficiency, calculated by a Monte Carlo method,[5] was overestimated using a radiation length of 62.5 g/cm^2 for electrons in polyethylene, whereas the correct value is about 45 g/cm^2.

In the recent experiment by Sard, Crowe, and Kruger (which has a sensitivity comparable to that of our second experiment though based on a quite different technique), three events have been recorded of the type searched for, whereas the expected background is estimated by the authors to be 0.23 event. This result yields for process (3) a branching ratio $R=(4\pm3)\times10^{-6}$ which is not inconsistent (as one can see also from Fig. 9) with our negative result. In this connection mention should perhaps be made of the fact that, as pointed out recently by Ernst,[8] if the intermediate boson can be adjusted to account for the absence of process (1), a branching ratio of the order of 10^{-6} would be expected for process (3).

On the basis of our negative result, it is possible to establish an upper limit for the coefficients which appear in the matrix elements derivable on phenomenological grounds[6,7] for the interaction represented by the Feynman diagram of Fig. 1. Indeed one can compute the branching ratio of process (3) relative to ordinary muon capture, using expressions of the transition probabilities given for the former process by Weinberg and Feinberg[6] and for the latter process by Primakoff.[17] Then

$$R=\frac{W(\mu^-+\mathrm{Cu}\rightarrow\mathrm{Cu}+e^-)}{W(\mu^-+\mathrm{Cu}\rightarrow\mathrm{Ni}+\nu)}=\frac{56(m_\mu c^2/\hbar)\alpha^5[\xi(m_\mu^2)]^2}{\gamma\Gamma(1,1)[1-\delta(A-Z)/2A]}, \tag{11}$$

where $m_\mu=103.8$ Mev is the total energy of the μ^- meson in the K orbit of the Cu nucleus; $\alpha=1/137$; γ is a parameter having the value 0.83[17]; $\Gamma(1,1)$ is the capture rate of the negative muon by a proton and is found to be ~260 sec^{-1} assuming the universal Fermi interaction; $\delta(A-Z)/2A$ is 0.82 for Cu and $\xi(m_\mu^2)$ has the same meaning as in reference 6. Inserting in Eq. (11) the numerical values, the negative result of our second experiment yields $[\xi(m_\mu^2)]^2<2\times10^{-18}$.

In terms of the dimensionless form factors relative to electric and magnetic monopole and dipole transitions, the quantity $\xi(m_\mu^2)$ can be explicitly written as[6]

$$[\xi(m_\mu^2)]^2=|f_{E0}(m_\mu^2)+f_{M1}(m_\mu^2)|^2+|f_{E1}(m_\mu^2)+f_{M0}(m_\mu^2)|^2. \tag{12}$$

The upper limit established[2] for the branching ratio of process (1) implies that

$$|f_{E1}(0)|^2+|f_{M1}(0)|^2<10^{-21}.$$

Assuming on the basis of this inequality that these dipole terms can be neglected also in Eq. (12), one obtains

$$|f_{E0}(m_\mu^2)|^2+|f_{M0}(m_\mu^2)|^2<2\times10^{-18}.$$

ACKNOWLEDGMENTS

We wish to thank Professor R. Gatto and Dr. N. Cabibbo for many illuminating discussions on the theoretical aspects of this research. We are indebted to Professor G. Fidecaro for information and advice especially in the early stages of our work at CERN. Thanks are also due to Dr. R. C. Hanna for much help in the preparation and use of the electron beam mentioned in Sec. 4. It is finally a pleasure to acknowledge the cordial cooperation of Dr. A. Citron, Dr. E. G. Michaelis, and the members of their group who have contributed to the development of the high-intensity beam used in our second experiment.

[17] H. Primakoff, *Proceedings of the Fifth Annual Rochester Conference on High-Energy Nuclear Physics* (Interscience Publishers, Inc., New York, 1955), p. 174.